

# Berry Phase of Bloch States through Modular Symmetries

Emanuele Maggio\*

*Mathematical and Physical Sciences for Advanced Materials and Technologies (MPHS) Cluster,  
Scuola Superiore Meridionale, largo San Marcellino, 10, 80127 Naples, Italy*

E-mail: emanuele.maggio@gmail.com

Submitted to: *Communications Physics*

## Abstract

The theoretical identification of crystalline topological materials has enjoyed sustained success in simplified materials models, often by singling out discrete symmetry operations protecting the topological phase. When band structure calculations of realistic materials are considered, complications often arise owing to the requirement of a consistent gauge in the Brillouin zone, or down to the fineness of its sampling. Yet, the Berry phase, acting as topological label, encodes geometrical properties of the system, and it should be easily accessible. Here, an expression for the Berry phase is obtained, thanks to analytical Bloch states constructed from an infinite series of Gaussian type orbitals. Two contributions in the Berry phase are identified, with one having an immediate geometric interpretation, being equal to the Zak phase. Eigenvalues of a modular symmetry, considered here for the first time in the context of crystalline solid state systems, are put in correspondence with the Zak phase: modular symmetries allow to define a non-trivial action for the spatial inversion also when the system does not have an inversion centre. The approach is showcased for the non-centrosymmetric space group no. 22 ( $F2\bar{2}2$ ), which is known to host symmetry equivalent Bloch states that can be distinguished by their Berry phase.

# 1 Introduction

The facile identification of crystalline topological systems has taken advantage of symmetry considerations,<sup>1–9</sup> with topological invariants being defined on the score of symmetry eigenvalue conservation. The prime example is the  $\mathbb{Z}_2$  invariant, that for centrosymmetric systems takes a particularly straightforward formulation<sup>10,11</sup> and which is related to other integral topological invariants.<sup>12,13</sup> For crystalline systems without inversion symmetry, their characterisation in the presence of time-reversal symmetry is more convoluted, as there is no easy formula that allow to distinguish topologically non-trivial band structures.<sup>14</sup> This has prompted the proliferation of computational schemes either relying on other symmetries protecting the topological phase,<sup>2,4,15–17</sup> or based on a particular representation of the materials' electronic structure. In the latter category one finds methods explicitly based on a localised Wannier representation<sup>18–21</sup> or elementary band decompositions.<sup>22–24</sup>

The implementation of either method is not without challenges: to track the evolution of the Wannier charge centre, for instance, it is necessary to finely sample the Brillouin zone as the dependence on the wavevector can only be computed numerically, whereas the framework of topological quantum chemistry<sup>24,25</sup> requires a smooth gauge along the band dispersion in order to consistently evaluate the transformation character of Bloch states (BSs) under symmetry operations of the local symmetry group for different wavevectors. Furthermore, the occurrence of fragile topological bands,<sup>26</sup> for which a Wannier representation, originally obstructed, can be realised by supplying additional degrees of freedom, leads to a determination of the topological nature of the band structure that is not stable against the addition of a topologically trivial set of bands. This phenomenon is at odds with the mathematical properties of the (first and second) Stiefel-Whitney classes which indicate an obstruction to orientability in the case of spinless, time-reversal invariant fermions or an obstruction to defining a spin structure as a function of the wavevector. The first and second Stiefel-Whitney numbers have been related to the Berry phase and the Wilson loop, respectively.<sup>27</sup>

In this Communication I am considering time-reversal invariant spinless BSs for which the calculation of the Berry phase is sufficient to characterise topologically inequivalent electronic

bands. In particular, I am going to derive an analytical expression for the Berry phase and apply it to the case of space group (SG) no. 22, which is a classic example<sup>28,29</sup> where symmetry-equivalent Bloch states are not physically equivalent, *i.e.* they can only be distinguished by their Berry phase. The analytical calculation of the Berry phase is made possible by a recent development<sup>30</sup> which allows to express the BS as an analytic (in fact entire) complex function and to retain the local information of the Gaussian type orbital (GTO) from which the BS is formed.

Alternative approaches to the classification of topological materials include their characterisation in terms of symmetry indicators,<sup>4,31</sup> which, unsurprisingly, turn out to be related to Berry phases (or differences thereof) along specific directions in the unit cell.<sup>32</sup> Unfortunately, the identification of topological crystalline materials can not rely exclusively on symmetry indicators, since the mapping from symmetry indicators to topological invariants is not bijective. In this Communication, a connection is established between the group of modular transformations of the BSs, whose action has never been considered before, with the expression for the Berry phase, thus paving the way to adjoining established symmetry indicators, derived only from space group operations, with additional ones stemming from modular symmetries.

## 2 Results

### 2.1 Analytical evaluation of the Berry phase for Riemann Bloch states

Riemann  $\vartheta$  functions have recently been proposed<sup>30</sup> to express BSs arising from GTOs centred at a given Wyckoff position (WP), indicated by the symbol  $\underline{w}$ ; the resulting BSs are immediately associated with a label conveying local information concerning the orbital's angular momentum ( $s, p, d, \dots$ ) and its location, by construction. The analytical expression for BSs depends on the complex variable  $\underline{z} = \underline{k} - \Omega \underline{\xi}$  in which the wavevector  $\underline{k}$  and the spatial coordinate  $\underline{\xi}$  are both referred to the conventional unit cell,  $\mathcal{U}$ . For an  $s$ -GTO (the only type of orbitals considered in this

Communication) the resulting Bloch state is:

$$\phi_{\underline{k}}(\xi|\underline{w}, \Omega) = N_{\underline{k}} e^{i\pi\xi \cdot \Omega \xi} e^{-2i\pi \underline{w} \cdot \underline{k}} \vartheta \begin{bmatrix} \underline{w} \\ 0 \end{bmatrix} (\underline{k} - \Omega \xi | \Omega), \quad (1)$$

where the Riemann  $\vartheta$  function with characteristics is defined in Sec. 4.2 and  $N_{\underline{k}}$  is a (wavevector dependent) normalisation constant. For notational convenience, I am suppressing the dependence on the Gaussian broadening  $\beta$  as it is implicit in the period matrix  $\Omega$ . To derive an analytical expression for the Berry phase and connection, the latter is assumed diagonal, *i.e.*  $\Omega = \tau \text{diag}(a^2, b^2, c^2)$  with  $a, b, c$  lattice constants and  $\tau = \frac{i\beta}{\pi}$ , in which case the Riemann  $\vartheta$  function reduces to the product of one-dimensional Jacobi functions (defined in Sec. 4.1) in each coordinate. Riemann and Jacobi functions will be distinguished by their vector or scalar input variables, respectively, although different notations for the two functions are common in the literature.<sup>33–35</sup>

Factorisation of the BS and orthogonality of the conventional crystal coordinates imply that for the normalisation constant  $N_{\underline{k}}$  one has:  $N_{\underline{k}}^2 = |T| \frac{1}{S_{\underline{k}}} = |T| \frac{1}{S_{k^1} S_{k^2} S_{k^3}}$ , which derives from the normalisation condition  $N_{\underline{k}}^2 \langle \tilde{\phi}_{\underline{k}} | \tilde{\phi}_{\underline{k}} \rangle = 1$ , with  $\tilde{\phi}$  being the unnormalised BS and the bracket  $\langle \bullet | \bullet \rangle$  indicating spatial integration over  $\mathcal{U}$ . In the following the determinant of the matrix  $T$  containing the Bravais lattice basis vectors is omitted in the expression for the one-dimensional component  $N_{k^\mu} = (S_{k^\mu})^{-\frac{1}{2}}$ . The "directional" superscript  $\mu$  will be dropped in the following, if this causes no misunderstanding.

The expression for the overlap  $S_k$  of a  $\vartheta$  function with respect to one coordinate (with lattice constant  $a$  along that direction), derived in Sec. 4.2, is given by another  $\vartheta$  function with scaled period  $\omega = \frac{1}{2}\tau a^2$ :

$$S_k = \sqrt{\frac{\pi}{2\beta}} \vartheta(k | \frac{1}{2}\tau a^2). \quad (2)$$

Two considerations emerge from Eq. 2 above: first, the explicit dependence on the wavevector implies that  $\nabla_{\underline{k}} \langle \phi_{\underline{k}} | \phi_{\underline{k}} \rangle \neq 0$  and consequently the Berry connection  $\mathcal{A}_{\underline{k}} \equiv i \langle u_{\underline{k}} | \nabla_{\underline{k}} u_{\underline{k}} \rangle$  is not

purely real on general grounds (*vide infra* for the definition of  $u_{\underline{k}}$ , the BS's periodic component). In Sec. 4.1 it is shown that for  $s$ -type BSs the imaginary contribution vanishes, however I can anticipate that careful analysis is necessary for BSs of higher orbital momentum, which will be reported elsewhere. Second, the BS is well defined as the normalisation constant does not vanish anywhere in the Brillouin zone: this descends from the zeros of a  $\vartheta$  function being located at  $\frac{1}{2} + \frac{1}{2}\omega + \Lambda$ , where  $\Lambda$  is the complex lattice generated by  $(1, \omega)$ .<sup>33,34,36</sup>

To evaluate the Berry connection, the periodic component of the BS  $u_{\underline{k}} = e^{-2i\pi\underline{\xi}\cdot\underline{k}} \phi_{\underline{k}}$  is introduced and the evaluation of its derivative  $\frac{\partial}{\partial k^\mu} u_{\underline{k}}$  is reported in [SI]. A crucial ingredient is the derivative of the normalisation constant:

$$\frac{\partial}{\partial k} N_k = -\frac{1}{2} N_k \frac{\partial}{\partial k} (\ln S_k) = -\frac{1}{2} N_k \frac{\vartheta'(k|\frac{1}{2}\tau a^2)}{\vartheta(k|\frac{1}{2}\tau a^2)}, \quad (3)$$

which leads to the presence of two components in the Berry connection, namely the "dissipative" and "geometrical" component:

$$\left\langle u_{\underline{k}} \left| \frac{\partial}{\partial k^\mu} u_{\underline{k}} \right. \right\rangle = -\frac{1}{2} \left[ \frac{\vartheta'(k^\mu|\frac{1}{2}\tau a^2)}{\vartheta(k^\mu|\frac{1}{2}\tau a^2)} + 4\pi i \langle \underline{e}^\mu, \underline{w} \rangle \right], \quad (4)$$

with the geometrical component consisting of the inner product  $\langle \underline{e}^\mu, \underline{w} \rangle$  between the direction with respect to which the derivative is taken and the Wyckoff position, whereas the expression for the dissipative component varies with the type of GTOs generating the BS; for  $s$ -GTOs it is given by the logarithmic derivative of the overlap function in Eq. 2.

From Eq. 4 it is immediately apparent that the Berry connection is a closed differential form (its curl evaluates to zero), and, with its integration in the Brillouin zone being path independent, it follows that its integral over a closed loop evaluates to zero identically. Therefore, the Berry phase can be evaluated meaningfully by considering as endpoints of the integration path (high symmetry) wavevectors on opposite faces of the Brillouin zone (that are identified under periodic boundary conditions), or an open path in the Brillouin zone, with the latter not being invariant under SG symmetries in general. Also, with the Berry curvature  $\mathcal{F} = \nabla_{\underline{k}} \times \mathcal{A}_{\underline{k}}$  being equal to zero, it

follows that the invariant introduced in ref.<sup>37</sup> reduces in this gauge to the exponential of the Berry phase.

The translational invariance of the  $\vartheta$  functions with respect to the wavevector allows one to fix the integration interval as  $[0, m]$ . If the integral is evaluated along the direction  $\underline{e}^\mu$  the Berry phase evaluates as

$$i\gamma(m) = \int_0^m dk^\mu \frac{1}{2} \left[ \frac{\vartheta'(k^\mu | \frac{1}{2}\tau a^2)}{\vartheta(k^\mu | \frac{1}{2}\tau a^2)} + 4\pi i (\underline{e}^\mu \cdot \underline{w}) \right] \quad (5)$$

the geometric component evaluates straightforwardly to  $2\pi i m (\underline{e}^\mu \cdot \underline{w})$ , while the dissipative component integrates to zero for the example considered in the next section. Note that if the upper integration limit is not an integer, as it might happen if an open path in reciprocal space is considered for primitive Bravais lattices, the dissipative component of the Berry connection may not vanish in general.

## 2.2 Application to symmetry-indistinguishable bands in SG no. 22 (F222)

To showcase that the action of modular symmetries can be successfully exploited to connote the distinct topological nature of electronic bands, the case of SG no. 22 (F222) is now considered. This space group has emerged as an early exception to the paradigm of a symmetry based classification of band representations, since the symmetry equivalent WPs give out physically non-equivalent band representations,<sup>38</sup> as they are associated to different values for the Berry phase.<sup>29</sup>

The WPs considered are indicated by the symbol  $\underline{w}_\alpha$  with  $\alpha \in \{a, b, c, d\}$ ; their multiplicity is four, *i.e.* under the action of space group operations there are four equivalent coordinates for each WP, belonging to the same orbit, indicated by  $\{\underline{w}_\alpha\}$ . The equivalent coordinates in each WP are reported in Fig. 1 panel (a). Space group elements that keep each coordinate fixed form the stabiliser group,  $\text{Stab}(\underline{w}_\alpha)$ , of the WP. For the four positions  $a, b, c, d$  we have that the stabilisers are all isomorphic and pairwise equal, *i.e.*  $\text{Stab}(\underline{w}_\alpha) \cong (\mathbb{Z}_2 \times \mathbb{Z}_2)$  and  $\text{Stab}(\underline{w}_a) = \text{Stab}(\underline{w}_b)$ ,  $\text{Stab}(\underline{w}_c) = \text{Stab}(\underline{w}_d)$ . Since the intersection of WPs' orbits is empty, it follows that the union of

their stabilisers can not be a finite subgroup of the space group, so it must contain a lattice translation.<sup>39</sup> This property characterises maximal WPs, and the corresponding band representations are elementary<sup>40</sup> owing to the stabilisers being Abelian. In such a case, the global band structure connectivity is determined by group-theoretical arguments (the so-called compatibility relations) if one knows which WPs partake in the material’s electronic structure and BSs’ transformation properties are thus fixed.<sup>41</sup> For the space group considered here, symmetry operations can not distinguish BSs pertaining to WPs in either pair  $(a, b)$  or  $(c, d)$ , then the determination of the band structure connectivity requires additional, topological, labels, provided by Berry phases.

The Berry phase is computed according to Eq. 5, with the choice of  $\underline{e}^\mu = \underline{e}^3$  along the  $\underline{k}_Z$  direction in reciprocal space, shown by a dashed line in Fig. 1 panel (b); the translational invariance of the  $\vartheta$  function with respect to the wavevector allows to fix the lower integration limit at the  $\Gamma$  point and by setting  $m = 2, 1$ , respectively, one evaluates the integral in Eq. 5 along a closed loop or along the open path  $\Gamma - Z$ , which reproduces previous results<sup>29</sup> reported in Tab. 1.

Next, I am considering the action of the inversion symmetry  $\mathcal{P}$ . Even though the space group is not centrosymmetric, the inversion is an element of the modular group (defined in [SI]) acting on  $\vartheta$  functions and modular forms. The symmetry eigenvalue for the modular component of the BS can, therefore, be estimated and it is found to coincide with  $e^{i\gamma}$ , thus providing an unexpected link between a topological invariant and a class of modular symmetries.

First, let’s examine the Wyckoff positions  $\underline{w}_\alpha$  that are shown in Fig. 1 panel (a) within the unit cell and in its image generated by the inversion symmetry  $\mathcal{P}$ . Since  $\mathcal{P}$  is not a space group operation, the corresponding orbit of  $\underline{w}_\alpha$  (*i.e.*  $\mathcal{P}\underline{w}_\alpha$ ) will not belong, in general, to the sublattice generated by  $\{\underline{w}_\alpha\}$  under lattice translations. However, coordinates in the pair  $(a, b)$  are fixed under  $\mathcal{P}$ , whose action, instead, swaps coordinates belonging to the pair  $(c, d)$ ; hence the sublattices generated by  $\{\underline{w}_c\}$  and  $\{\underline{w}_d\}$  are identified under inversion. This behaviour is shared by BSs generated by GTOs located at WP coordinates  $\{\underline{w}_\alpha\}$  (synthetically referred to in the following with the notation BSs @  $\{\underline{w}_\alpha\}$ ) and it is analysed in Sec. SI.1, where it is shown that the inversion symmetry applied to the BSs returns a trivial eigenvalue, which therefore cannot serve as a topological

label for the dispersion involved; the opposite is true when  $\mathcal{P}$  is applied to the *modular* component of the BSs.

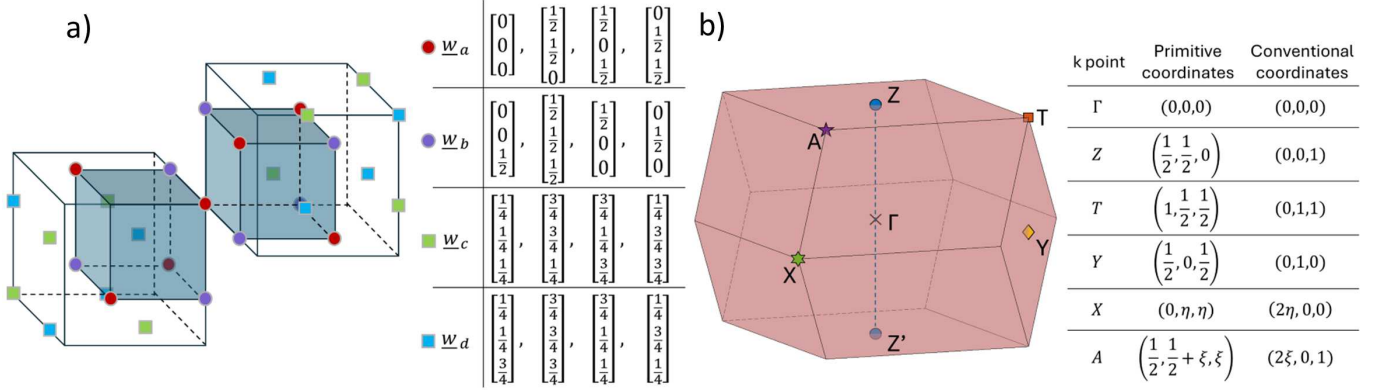


Figure 1: High symmetry points in direct (panel a) and reciprocal (panel b) space for space group  $F222$  no. 22. In panel a) the Wyckoff positions  $w_a$  to  $w_d$  are shown in the unit cell and in its image under inversion symmetry. The cubes with edge length  $\frac{1}{2}$  (shaded faces) and  $\frac{3}{4}$  (transparent faces) have been included as a guide to the eye. Wyckoff coordinates in the unit cell for each position are indicated. In panel b) the Brillouin zone corresponding to the choice of lattice parameters  $\frac{1}{a^2} = \frac{1}{b^2} + \frac{1}{c^2}$  is shown with lattice-dependent high-symmetry wavevector coordinates  $\eta = \frac{1}{4}(1 + (\frac{a}{b})^2) + (\frac{a}{c})^2$  and  $\xi = \frac{1}{4}(1 + (\frac{a}{b})^2) - (\frac{a}{c})^2$ .<sup>42</sup> The integration path for the calculation of the Berry phase carried out in the text is indicated by a dashed line.

To prove the claim above, recall that the action on the  $\vartheta$  functions evaluates as  $\mathcal{P} \left[ \vartheta \left[ \frac{w}{k} \right] (\underline{z}|\Omega) \right] = \vartheta \left[ \frac{w}{k} \right] (-\underline{z}|\Omega) = \vartheta \left[ \frac{-w}{-k} \right] (\underline{z}|\Omega)$ .<sup>30,36</sup> For the pair  $(a, b)$  the coordinates  $w_\alpha$  have integer or half-integer entries and the corresponding BSs are eigenfunctions of the inversion centre, with eigenvalue  $e_*(w_\alpha, \underline{k}) = (-1)^{4w_\alpha \cdot \underline{k}}$  for any  $\underline{k} \in \frac{1}{2}\mathbb{Z}^3$ ; the parity eigenvalue evaluates to  $+1$  at the  $Z$ -point, as reported in Tbl. 1. For the  $\vartheta$  functions with characteristics  $w_c$  or  $w_d$ , on the other hand, one has that the action of the inversion symmetry matches that on the corresponding sublattices generated by the WPs: a direct calculation shows that  $\vartheta \left[ \frac{-w_c}{-k} \right] (\underline{z}|\Omega) = \vartheta \left[ \frac{w_d - \frac{1}{2}}{k - 2\underline{k}} \right] (\underline{z}|\Omega) = (-1)^{4w_d \cdot \underline{k}} \vartheta \left[ \frac{w_d}{k} \right] (\underline{z}|\Omega) = e_*(w_d, \underline{k}) \vartheta \left[ \frac{w_d}{k} \right] (\underline{z}|\Omega)$ , for any  $\underline{k}$ -point with integer or half-integer coordinates. Hence, the  $\vartheta$  functions retain the action of the inversion symmetry on the two sublattices (with WPs  $w_c$  and  $w_d$  being swapped), and the corresponding symmetry eigenvalue is not affected, taking value  $-1$  in either case.

The Berry phase evaluated along the closed loop  $Z' - \Gamma - Z$  can be obtained by setting  $m = 2$

in Eq. 5 and the corresponding numerical values are reported in Tab. 1. In order to discriminate between the topologically distinct BSs, the Berry phase has to be evaluated on the open path  $\Gamma - Z$  (corresponding to  $m = 1$  in Eq. 5), or along any reciprocal lattice vector,<sup>29</sup> the parity of the representative  $\vartheta$  function evaluated at the "barycenter" of the dispersion (*i.e.* at the midpoint of the integration interval) again matches the computed values for the Berry phase. Next I am going to contrast the derivation above to a previously reported expression<sup>43</sup> obtained in a less general setting and compare the BSs features that are encoded in the Berry phase.

Table 1: Berry phase  $\gamma$  and parity eigenvalue computed for the constituent  $\vartheta$  functions of  $s$ -BSs located at the representative Wyckoff position coordinate  $\underline{w}_\alpha$  (reported in the first column of the list of Fig. 1). The parity eigenvalue is evaluated with  $\beta = \alpha$ ,  $j = 1$  for  $\alpha = a, b$  and  $\beta = d, c$ ,  $j = 2$  for  $\alpha = c, d$  respectively.

| $\alpha$ | $\gamma(2)$ | $e^{i\gamma}$ | $e_*(\underline{w}_\beta^{(j)}, k_Z)$ | $\gamma(1)$      | $e^{i\gamma(1)}$ | $e_*(\underline{w}_\beta^{(j)}, \frac{1}{2}k_Z)$ |
|----------|-------------|---------------|---------------------------------------|------------------|------------------|--|
| $a$      | 0           | 1             | 1                                     | 0                | 1                | 1  |
| $b$      | $2\pi$      | 1             | 1                                     | $\pi$            | -1               | -1   |
| $c$      | $\pi$       | -1            | -1                                    | $\frac{\pi}{2}$  | i                | i  |
| $d$      | $3\pi$      | -1            | -1                                    | $-\frac{\pi}{2}$ | -i               | -i   |

### 3 Discussion

The BSs considered are the result of a Bloch-Floquet transform<sup>44,45</sup> of a symmetric superposition of  $s$ -GTOs centred at the coordinates in  $\{\underline{w}_\alpha\}$ ,  $\alpha \in \{a, b, c, d\}$ . At the  $\Gamma$ -point all BSs transform like the trivial representation (see Tbl. S1 in SI), hence they are all invariant under SG symmetries. In Fig. 2 the section of the BSs along the plane  $\xi_2 = 0$  are reproduced, with  $\text{BS}@ \{\underline{w}_a\}$  and  $\text{BS}@ \{\underline{w}_b\}$  at the top and  $\text{BS}@ \{\underline{w}_c\}$ ,  $\text{BS}@ \{\underline{w}_d\}$  in the bottom row. The relative shift of the BSs associated to the two WPs pairs is evident from the pictures and stems from the same property of the constituent  $\vartheta$  functions, which is reflected by the parity eigenvalue of the  $\vartheta$  function evaluated at the  $Z$ -point (note that the BSs at  $\Gamma$  and  $Z$  are identical) and consistently, by the  $\gamma(2)$  values.

To get a more granular distinction between the states one has to evaluate  $\gamma(1)$  (in agreement with previous studies<sup>29,37</sup>) which is able to uniquely identify each of the BSs considered. To

interpret the values taken by the Berry phase let's start by considering the pair  $(a, b)$  in Fig.2, for which the Berry phase  $\gamma(1)$  takes real values. One readily identifies the translation by  $\frac{1}{2}\underline{e}^3$  as the symmetry breaking transformation (it is not an element of the SG) able to map  $\text{BS}@\{\underline{w}_a\}$  to  $\text{BS}@\{\underline{w}_b\}$ . The expression for the BSs is invariant by shifting the unit cell origin (as reported in Sec. 4.2 and previously shown<sup>30</sup>) hence the relative phase difference along the  $\xi_1$  and  $\xi_2$  directions (the latter shown in Fig. S1 in SI) connotes two physically inequivalent BSs. In contrast, for the case of  $\text{BS}@\{\underline{w}_c\}$  and  $\text{BS}@\{\underline{w}_d\}$  the Berry phase takes purely imaginary values and the two states, in fact, coincide.

A plausible explanation for the observed behaviour involves the relationship that has been established in this Communication between the Berry phase and system's symmetries. In general, the BSs form a basis for the symmetry invariant manifolds associated to irreducible representations of the local symmetry group of the wavevector. For the case at hand, all irreducible representations have real characters, and one is led to conjecture that the reality of the manifolds does not allow to tell apart (by the action of symmetry transformations) states that are associated with imaginary values taken by the Berry phase. It would be interesting to test this conjecture on the many pairs of (physically) inequivalent WPs identified in ref.<sup>37</sup> and see if for the case of complex characters, there is a symmetry operation able to distinguish BSs associated to imaginary values of the Berry phase.

As a final remark, note that the integrated expression for the geometric component in Eq. 5 is, one has to remark, identical to the one derived by Zak more than a quarter of a century ago;<sup>43</sup> in order to make a connection to the WP, in that work, it was assumed the presence of the inversion centre in a one-dimensional material model. Here, the derivation of the expression for the Berry phase is completely general and rests only on the expression for the BS in terms of Riemann  $\vartheta$  functions and on their peculiar property for the overlap integral, which is just another  $\vartheta$  function with scaled period. The resulting expression for the Berry phase is of general applicability and it can be fruitfully applied for the definition of new discrete topological invariants. Like many of them, the present topological invariant is protected by a symmetry of the electronic state, which

acts on the modular component of the BS.

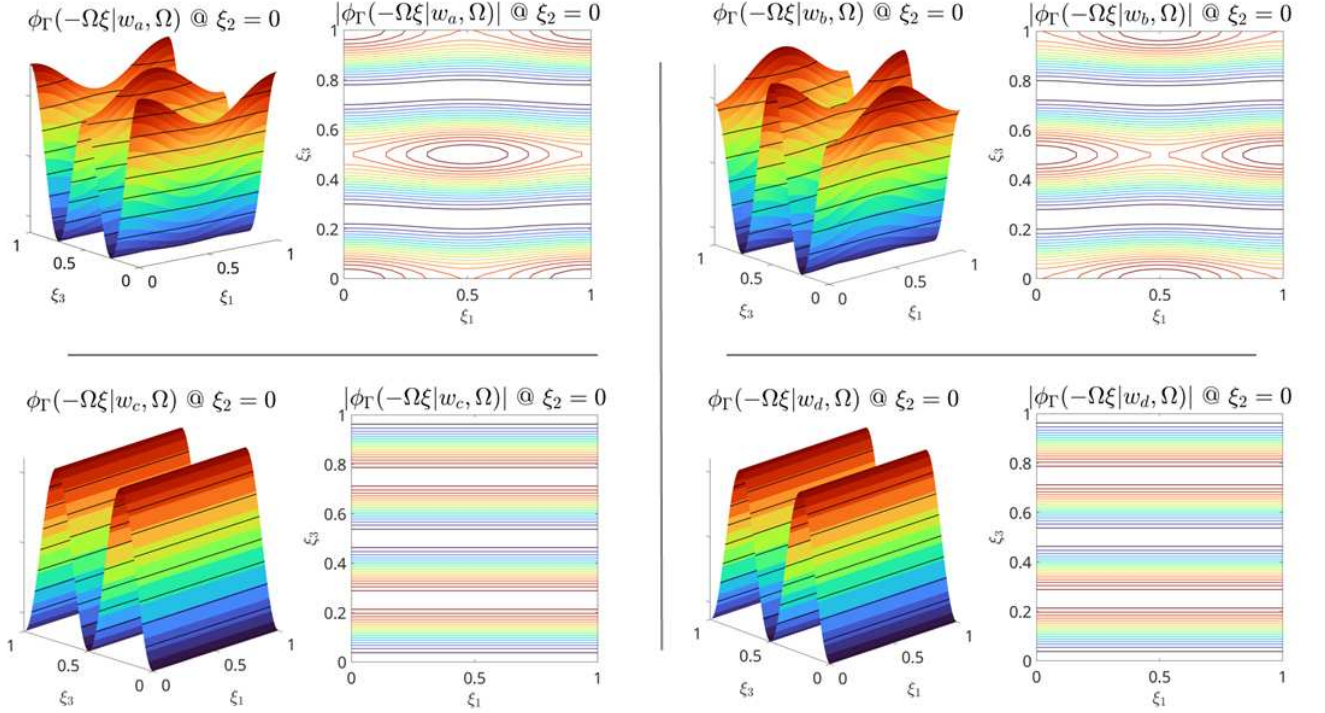


Figure 2: Bloch states @  $\{\underline{w}_\alpha\}$ ,  $\alpha \in \{a, b, c, d\}$ . Each panel shows the real part (left) and the absolute value of the BS in the plane  $\xi_2 = 0$ , the imaginary part of the Bloch states is zero at the  $\Gamma$ -point.

## 4 Methods

The numerical evaluation of  $\vartheta$  functions has been carried out as in Ref.<sup>30</sup>, omitting the normalisation constant for the GTOs. The approximation method banks on the pointwise approximation introduced in Ref.<sup>46</sup>, which allows to set the numerical error in the evaluation of the  $\vartheta$  function as an input parameter, here set to  $10^{-8}$ . The analytical expression for the overlap integral has been compared to the result of numerical integration using the built in trapezoid method implemented in MATLAB:<sup>47</sup> setting the lattice constants to the numerical values  $a = 1$ ,  $b = \frac{5}{4}$ ,  $c = \frac{5}{3}$ , the numerical approximation  $S^{(N)}$  to  $S$  already converges to the analytical value with an absolute error  $|S^{(N)} - S| \approx 10^{-11}$  for  $N \geq 5$ , for the BS  $\tilde{\phi}_\Gamma(\xi | \underline{w}_a, \tau \text{diag}(a^2, b^2, c^2))$ , with  $\tau = \frac{2i}{\pi}$ .

The assignment of a BS to an irreducible representation of the local symmetry group of the wavevector is carried out by evaluating the ratio  $\frac{F[\phi]}{\phi}$ , where  $F$  is the SG operation,<sup>30</sup> the result is compared with the character table reported in [SI].

In the rest of this section I am reporting the derivation of the salient results presented in the main text, together with the necessary definitions, starting with the integral of the Berry connection that is somewhat easier to derive.

## 4.1 Integration of the dissipative component of the Berry connection

Define the Jacobi  $\vartheta$  function as follows:

$$\vartheta(z|\omega) = \sum_{n=-\infty}^{+\infty} e^{i\pi\omega n^2} e^{2\pi i n z} = \sum_{n=-\infty}^{+\infty} v^{2n} q^{n^2}, \quad (6)$$

with  $z \in \mathbb{C}$  the argument, the parameter  $\omega \in \mathbb{C}$ ,  $\Im\{\omega\} > 0$  being the period and  $q = e^{i\pi\omega}$  typically referred to as the nome.<sup>35</sup> The Jacobi triple product states (see Ref.<sup>33</sup> Eq. 2.6.24 and Ref.<sup>35</sup> Eq. 20.5.9):  $\sum_{n=-\infty}^{+\infty} v^{2n} q^{n^2} = \prod_{n=1}^{+\infty} (1 - q^{2n})(1 + (v^2 + v^{-2})q^{2n-1} + q^{4n-2})$  which can be rewritten as  $q_0 \prod_{n=1}^{+\infty} c_n$ , with  $q_0 = \prod_{n=1}^{+\infty} 1 - q^{2n}$  and  $c_n(z) = 1 + 2 \cos(2\pi z)q^{2n-1} + q^{4n-2}$ . Then, for the ratio of the function and its derivative we have:

$$\frac{\vartheta'(z|\omega)}{\vartheta(z|\omega)} = \frac{\frac{d}{dz} \prod c_n(z)}{\prod c_n(z)} = \sum_{n=1}^{+\infty} \frac{c'_n}{c_n} = -4\pi \sin(2\pi z) \sum_n \frac{q^{2n-1}}{1 + 2 \cos(2\pi z)q^{2n-1} + q^{4n-2}} \quad (7)$$

and the integral over the real part of the complex variable  $\Re\{z\} = k$

$$\int_0^m dk \frac{\vartheta'(k|\omega)}{\vartheta(k|\omega)} = 2 \sum_n (-q)^{2n-1} 2\pi \int_0^m dk \frac{\sin(2\pi k)}{1 - 2 \cos(2\pi k)(-q)^{2n-1} + ((-q)^{2n-1})^2}$$

vanishes identically, since for a given value of  $n$  one has:

$$2\pi \int_0^m dk \frac{\sin(2\pi k)}{1 - 2a \cos(2\pi k) + a^2} = \int_0^{2\pi m} dx \frac{\sin(x)}{1 - 2a \cos(x) + a^2} = \frac{1}{2a} \int_{(1-a)^2}^{(1-a)^2} \frac{du}{u} = 0 \quad (8)$$

owing to the integration limits of the transformed integral coinciding for  $m \in \mathbb{Z}$ .

## 4.2 Overlap integral for s-GTO BSs

The Riemann  $\vartheta$  function with characteristics  $\underline{a}, \underline{b} \in \mathbb{R}^3$  is defined as:<sup>35,36</sup>

$$\vartheta \left[ \begin{matrix} \underline{a} \\ \underline{b} \end{matrix} \right] (\underline{z} | \Omega) = e^{i\pi \underline{a} \cdot \Omega \underline{a}} e^{2\pi i \underline{a} \cdot (\underline{z} + \underline{b})} \vartheta(\underline{z} + \Omega \underline{a} + \underline{b} | \Omega), \quad (9)$$

with  $\underline{z} \in \mathbb{C}^3$  and  $\Omega$  an element of the Siegel upper-half space, that is  $\Omega \in \mathbb{C}^{3 \times 3}$  is symmetric and its imaginary part is positive definite. The exponential terms in Eq. 9 ensure the translational invariance of the BS, which implies that for an  $s$ -BS one has  $\phi_k(\underline{\xi} | \underline{w}, \Omega) = \phi_k(\underline{\xi} - \underline{w} | \underline{0}, \Omega) = \varphi_k(\underline{\xi} - \underline{w} | \Omega)$ . If the overall BS factorises (as it happens for a diagonal period matrix  $\Omega$ ), then it is possible to evaluate the overlap integral analytically along each cartesian direction, with  $a$  the corresponding lattice parameter and  $W$  the Wyckoff position component in those coordinates. The expression for the overlap integral reads:

$$S_k(\tau a^2) = \int_0^a dx \tilde{\varphi}_{-k} \left( \frac{1}{a}(x - W) | \tau a^2 \right) \tilde{\varphi}_k \left( \frac{1}{a}(x - W) | \tau a^2 \right) \quad (10)$$

where the reality of the Gaussians allows one to consider the BS at momentum  $-k$  in stead of the complex conjugate function.<sup>48</sup> Inserting the definition in Eq. 6 one writes the integral as:

$$\begin{aligned} S_k(\tau a^2) &= \sum_{m,n \in \mathbb{Z}} e^{2\pi i k(n-m)} e^{-\beta a^2(n^2+m^2)} \int_0^a dx e^{-2\beta(x-W)^2} e^{2\beta a(n+m)(x-W)} \\ &= \sum_{m,n \in \mathbb{Z}} e^{2\pi i k(n-m)} e^{-\beta a^2(n^2+m^2)} e^{\frac{1}{2}\beta a^2(m+n)^2} \int_0^a dx e^{-2\beta(x-W-\frac{a}{2}(n+m))^2} \\ &= \sum_{m,n \in \mathbb{Z}} e^{2\pi i k(n-m)} e^{-\frac{1}{2}\beta a^2(n-m)^2} \int_0^a dx e^{-2\beta(x-W-\frac{a}{2}(n+m))^2} \\ &= \sum_{s=-\infty}^{+\infty} e^{2\pi i ks} e^{-\frac{1}{2}\beta a^2 s^2} \sum_{m=-\infty}^{+\infty} \int_0^a dx e^{-2\beta(x-W-am-\frac{1}{2}as)^2} \end{aligned} \quad (11)$$

where in going to the last line above we have introduced the summation index  $s = n - m$ . Now we continue with a change of variable that shifts the integral:  $\tilde{x} = x - am$ , thus leading to an integration interval  $[-am, a(1 - m)]$ , which, as the summation index is varied, ends up spanning the whole real axis, thus:

$$\begin{aligned}
S_k(\tau a^2) &= \sum_{s=-\infty}^{+\infty} e^{2\pi iks} e^{-\frac{1}{2}\beta a^2 s^2} \sum_{m=-\infty}^{+\infty} \int_{-am}^{a(1-m)} d\tilde{x} e^{-2\beta(\tilde{x}-W-\frac{1}{2}as)^2} \\
&= \sum_{s=-\infty}^{+\infty} e^{2\pi iks} e^{-\frac{1}{2}\beta a^2 s^2} \int_{-\infty}^{+\infty} d\tilde{x} e^{-2\beta(\tilde{x}-W-\frac{1}{2}as)^2} \\
&= \sum_{s=-\infty}^{+\infty} e^{2\pi iks} e^{-\frac{1}{2}\beta a^2 s^2} \int_{-\infty}^{+\infty} dy e^{-2\beta y^2} = \sqrt{\frac{\pi}{2\beta}} \sum_{n=-\infty}^{+\infty} e^{2\pi ikn} e^{-\frac{1}{2}\beta a^2 n^2} \\
&= \sqrt{\frac{\pi}{2\beta}} \vartheta\left(k \left| \frac{i\beta}{2\pi} a^2 \right. \right) = \sqrt{\frac{\pi}{2\beta}} \vartheta\left(k \left| \frac{1}{2} \tau a^2 \right. \right). \tag{12}
\end{aligned}$$

## Acknowledgement

The author acknowledges funding from the Scuola Superiore Meridionale per DM MUR n. 581 June 24, 2022.

## Supporting Information Available

The following file is available free of charge.

- SuppInfo: contains the definition of the Modular group and characterisation of the BS under inversion symmetry, character table and additional derivations.

## References

- (1) Slager, R. J.; Mesaros, A.; Juričić, V.; Zaanen, J. The space group classification of topological band-insulators. *Nature Physics* **2013**, *9*, 98–102.

(2) Po, H. C.; Vishwanath, A.; Watanabe, H. Symmetry-based indicators of band topology in the 230 space groups. *Nature Communications* **2017**, *8*, 50.

(3) Chang, G.; Wieder, B. J.; Schindler, F.; Sanchez, D. S.; Belopolski, I.; Huang, S.-M.; Singh, B.; Wu, D.; Chang, T.-R.; Neupert, T.; Xu, S.-Y.; Lin, H.; Hasan, M. Z. Topological quantum properties of chiral crystals. *Nature Materials* **2018**, *17*, 978–985.

(4) Song, Z.; Zhang, T.; Fang, Z.; Fang, C. Quantitative mappings between symmetry and topology in solids. *Nature Communications* **2018**, *9*, 3530.

(5) Yoshida, T.; Daido, A.; Kawakami, N.; Yanase, Y. Efficient method to compute Z4 indices with glide symmetry and applications to the Möbius materials CeNiSn and UCoGe. *Physical Review B* **2019**, *99*, 235105.

(6) Zhao, Y. X.; Huang, Y.-X.; Yang, S. A. Z2-projective translational symmetry protected topological phases. *Physical Review B* **2020**, *102*, 161117.

(7) Kim, H.; Shiozaki, K.; Murakami, S. Glide-symmetric magnetic topological crystalline insulators with inversion symmetry. *Physical Review B* **2019**, *100*, 165202.

(8) Kim, H.; Murakami, S. Glide-symmetric topological crystalline insulator phase in a nonprimitive lattice. *Physical Review B* **2020**, *102*, 195202.

(9) Wang, Z.; Wang, X.; Hu, Z.; Bongiovanni, D.; Jukić, D.; Tang, L.; Song, D.; Morandotti, R.; Chen, Z.; Buljan, H. Sub-symmetry-protected topological states. *Nature Physics* **2023**, *19*, 992–998.

(10) Fu, L.; Kane, C. L.; Mele, E. J. Topological Insulators in Three Dimensions. *Physical Review Letters* **2007**, *98*, 106803.

(11) Fu, L.; Kane, C. L. Topological insulators with inversion symmetry. *Physical Review B* **2007**, *76*, 045302.

(12) Fu, L.; Kane, C. L. Time reversal polarization and a Z2 adiabatic spin pump. *Physical Review B* **2006**, *74*, 195312.

(13) Wang, Z.; Qi, X.-L.; Zhang, S.-C. Equivalent topological invariants of topological insulators. *New Journal of Physics* **2010**, *12*, 065007.

(14) Fu, L. Topological Crystalline Insulators. *Physical Review Letters* **2011**, *106*, 106802.

(15) Zhang, T.; Jiang, Y.; Song, Z.; Huang, H.; He, Y.; Fang, Z.; Weng, H.; Fang, C. Catalogue of topological electronic materials. *Nature* **2019**, *566*, 475–479.

(16) Tang, F.; Po, H. C.; Vishwanath, A.; Wan, X. Comprehensive search for topological materials using symmetry indicators. *Nature* **2019**, *566*, 486–489.

(17) Xiao, J.; Yan, B. First-principles calculations for topological quantum materials. *Nature Reviews Physics* **2021**, *3*, 283–297.

(18) Soluyanov, A. A.; Vanderbilt, D. Computing topological invariants without inversion symmetry. *Physical Review B* **2011**, *83*, 235401.

(19) Yu, R.; Qi, X. L.; Bernevig, B. A.; Fang, Z.; Dai, X. Equivalent expression of Z2 topological invariant for band insulators using the non-Abelian Berry connection. *Physical Review B* **2011**, *84*, 075119.

(20) Wu, Q.; Zhang, S.; Song, H.-F.; Troyer, M.; Soluyanov, A. A. WannierTools: An open-source software package for novel topological materials. *Computer Physics Communications* **2018**, *224*, 405–416.

(21) Gresch, D.; Autès, G.; Yazyev, O. V.; Troyer, M.; Vanderbilt, D.; Bernevig, B. A.; Soluyanov, A. A. Z2Pack: Numerical implementation of hybrid Wannier centers for identifying topological materials. *Physical Review B* **2017**, *95*, 075146.

(22) Zak, J. Band representations and symmetry types of bands in solids. *Physical Review B* **1981**, *23*, 2824–2835.

(23) Michel, L.; Zak, J. Connectivity of energy bands in crystals. *Physical Review B* **1999**, *59*, 5998–6001.

(24) Bradlyn, B.; Elcoro, L.; Cano, J.; Vergniory, M. G.; Wang, Z.; Felser, C.; Aroyo, M. I.; Bernevig, B. A. Topological quantum chemistry. *Nature* **2017**, *547*, 298–305.

(25) Cano, J.; Bradlyn, B. Band Representations and Topological Quantum Chemistry. *Annual Review of Condensed Matter Physics* **2021**, *12*, 225–246.

(26) Po, H. C.; Watanabe, H.; Vishwanath, A. Fragile Topology and Wannier Obstructions. *Physical Review Letters* **2018**, *121*, 126402.

(27) Ahn, J.; Kim, D.; Kim, Y.; Yang, B.-J. Band Topology and Linking Structure of Nodal Line Semimetals with Z2 Monopole Charges. *Physical Review Letters* **2018**, *121*, 106403.

(28) Zak, J. In *Group Theoretical Methods in Physics, Lecture Notes in Physics*; Dodonov, V., Man'ko, V., Eds.; Springer Berlin Heidelberg, 1991; Vol. 382; pp 581–587.

(29) Michel, L.; Zak, J. Physical equivalence of energy bands in solids. *Epl* **1992**, *18*, 239–244.

(30) Maggio, E. Exploiting  $\vartheta$ -functions for the identification of topological materials. *AIP Advances* **2025**, *15*, 085107.

(31) Po, H. C. Symmetry indicators of band topology. *Journal of Physics: Condensed Matter* **2020**, *32*, 263001.

(32) Song, Z.; Zhang, T.; Fang, C. Diagnosis for Nonmagnetic Topological Semimetals in the Absence of Spin-Orbital Coupling. *Physical Review X* **2018**, *8*, 31069.

(33) D'Hoker, E.; Kaidi, J. *Modular Forms and String Theory*; Cambridge University Press, 2024.

(34) Diamond, F.; Shurman, J. *A First Course in Modular Forms*; Springer New York, 2005; Vol. 228.

(35) Olver, F. W. J.; Lozier, D. W.; Boisvert, R. F.; Clark, C. W., Eds. *NIST Handbook of Mathematical Functions*; Cambridge University Press, 2010; pp xv–951.

(36) Mumford, D. *Tata Lectures on Theta I*; Birkhäuser, 1983.

(37) Cano, J.; Elcoro, L.; Aroyo, M. I.; Bernevig, B. A.; Bradlyn, B. Topology invisible to eigenvalues in obstructed atomic insulators. *Physical Review B* **2022**, *105*, 125115.

(38) Bacry, H.; Michel, L.; Zak, J. Symmetry and analyticity of energy bands in solids. *Physical Review Letters* **1988**, *61*, 1005–1008.

(39) Fuksa, J.; Engel, P. Derivation of Wyckoff positions of N-dimensional space groups. Theoretical considerations. *Acta Crystallographica Section A* **1994**, *50*, 778–792.

(40) Michel, L.; Zak, J. Elementary energy bands in crystals are connected. *Physics Report* **2001**, *341*, 377–395.

(41) Zeiner, P.; Dirl, R.; Davies, B. L. Comments on the decomposition of the regular representation of crystallographic space groups into band representations. *Journal of Physics A: Mathematical and General* **2000**, *33*, 1631–1646.

(42) Maggio, E.; Smolyanyuk, A.; Tomczak, J. M. Local symmetry groups for arbitrary wavevectors. *Journal of Physics A: Mathematical and Theoretical* **2023**, *56*, 455307.

(43) Zak, J. Berry’s phase for energy bands in solids. *Physical Review Letters* **1989**, *62*, 2747–2750.

(44) Kuchment, P. A. Floquet theory for partial differential equations. *Russian Mathematical Surveys* **1982**, *37*, 1–60.

(45) Dirl, R.; Payer, K.; Davies, B. L. Symmetrized plane waves: 1. Symmorphic space groups. *Computer Physics Communications* **1996**, *98*, 52–72.

(46) Deconinck, B.; Heil, M.; Bobenko, A.; van Hoeij, M.; Schmies, M. Computing Riemann theta functions. *Mathematics of Computation* **2003**, *73*, 1417–1443.

(47) The MathWorks Inc. (2024). MATLAB version: 24.2.0 (R2024b).

(48) Zeiner, P.; Dirl, R.; Davies, B. L. Bloch and Wannier functions composed of Gaussian orbitals—analyticity, localization, and expectation values. *Journal of Mathematical Physics* **1998**, *39*, 2437–2454.

# Supporting Information:

## Berry Phase of Bloch States through Modular Symmetries

<sup>1</sup>

Emanuele Maggio\*

*Mathematical and Physical Sciences for Advanced Materials and Technologies (MPHS) Cluster,  
Scuola Superiore Meridionale, largo San Marcellino, 10, 80127 Naples, Italy*

E-mail: emanuele.maggio@gmail.com

## <sup>2</sup> 1 Modular group and inversion symmetry characterisation

<sup>3</sup> The Riemann  $\vartheta$  functions in the main text retain a parametric dependence on the period matrix

<sup>4</sup>  $\Omega \in \mathbb{C}^{g \times g}$  which is a purely imaginary matrix with imaginary part being symmetric and positive

<sup>5</sup> definite. The space of such matrices is denoted by  $\mathcal{H}_g$  in the following. The modular group

<sup>6</sup>  $Sp(2g, \mathbb{R})$  is defined as the group of matrices with real entries of the form  $\begin{pmatrix} A & B \\ C & D \end{pmatrix}$  that preserve

<sup>7</sup> the symplectic form  $\begin{pmatrix} 0 & \mathbb{I}_g \\ -\mathbb{I}_g & 0 \end{pmatrix}$ , that is for which the identity

$$\begin{pmatrix} A & C \\ B & D \end{pmatrix}^t \begin{pmatrix} 0 & \mathbb{I}_g \\ -\mathbb{I}_g & 0 \end{pmatrix} \begin{pmatrix} A & B \\ C & D \end{pmatrix} = \begin{pmatrix} 0 & \mathbb{I}_g \\ -\mathbb{I}_g & 0 \end{pmatrix}$$

<sup>8</sup> holds. The group is generated by the elements

$$S = \begin{pmatrix} A & 0 \\ 0 & (A^t)^{-1} \end{pmatrix} \text{ and } T = \begin{pmatrix} \mathbb{I}_g & B \\ 0 & \mathbb{I}_g \end{pmatrix}$$

<sup>9</sup> that act on the period matrix  $\Omega \in \mathcal{H}_g$  as follows:  $S : \Omega \mapsto A\Omega A^t$  and  $T : \Omega \mapsto \Omega + B$ .

<sup>10</sup> The action of the modular group on the pair  $(\underline{z}, \Omega) \in \mathbb{C}^g \times \mathcal{H}_g$  is:<sup>S1</sup>  $(\underline{z}, \Omega) \mapsto (((C\Omega + D)^t)^{-1}, (A\Omega + B)(C\Omega + D)^{-1})$ , that allows to define the transformation law for  $\vartheta$  functions for  
<sup>11</sup> a generic  $\mathcal{R} \in Sp(2g, \mathbb{R})$ :

$$\mathcal{R}[\vartheta(\underline{z}|\Omega)] = \vartheta\left(((C\Omega + D)^t)^{-1}\underline{z} \mid (A\Omega + B)(C\Omega + D)^{-1}\right). \quad (1)$$

<sup>13</sup> Obviously  $\mathcal{R}$  can be specified as the inversion symmetry  $\mathcal{P}$ , in which case the action reduces  
<sup>14</sup> to  $\mathcal{P}[\vartheta(\underline{z}|\Omega)] = \vartheta(-\underline{z}|\Omega)$ . From the series expansion in Sec. 4.1 in the main text one has that  
<sup>15</sup>  $\vartheta(-\underline{z}|\Omega) = \vartheta(\underline{z}|\Omega)$ , whereas for  $\vartheta$  functions with characteristics a simple calculation<sup>S2</sup> shows  
<sup>16</sup> that  $\vartheta\left[\frac{w}{k}\right](-\underline{z}|\Omega) = \vartheta\left[\frac{-w}{-k}\right](\underline{z}|\Omega)$ .

<sup>17</sup> The action of the inversion symmetry can be evaluated on the Bloch states in the main text, for  
<sup>18</sup> which an explicit definition involving all coordinates in the Wyckoff position is:  $\phi_{\underline{k}}(\xi|\{w_\alpha\}, \Omega) =$   
<sup>19</sup>  $\sum_{i=1}^4 \phi_{\underline{k}}(\xi|w_\alpha^{(i)}, \Omega)$ , with  $i$  running over the elements in the orbit  $\{w_\alpha\}$ . Starting with the case  
<sup>20</sup>  $\alpha = c$ , we have that

$$\begin{aligned} \mathcal{P}[\phi_{\underline{k}}(\xi|\{w_c\}, \Omega)] &= \sum_{i=1}^4 \phi_{\underline{k}}(-\xi|w_c^{(i)}, \Omega) = \sum_{i=1}^4 e^{i\pi\xi \cdot \Omega\xi} e^{-2i\pi w_c^{(i)} \cdot \underline{k}} \vartheta\left[\frac{w_c^{(i)}}{k}\right](-\underline{z}|\Omega) \\ &= \sum_{i=1}^4 e^{i\pi\xi \cdot \Omega\xi} e^{-2i\pi w_c^{(i)} \cdot \underline{k}} \vartheta\left[\frac{-w_c^{(i)}}{-k}\right](\underline{z}|\Omega) \\ &= \sum_{i=1}^4 e^{i\pi\xi \cdot \Omega\xi} e^{-2i\pi w_c^{(i)} \cdot \underline{k}} e^{-4i\pi w_d^{(j)} \cdot \underline{k}} \vartheta\left[\frac{w_d^{(j)}}{k}\right](\underline{z}|\Omega) \end{aligned}$$

<sup>21</sup> where the wavevector coordinates appear as a characteristic of the  $\vartheta$  function, thus  $\underline{z} = -\Omega\xi$ ; in  
<sup>22</sup> going to the last line of the equation above the correspondence between coordinates in  $\{w_c\}$  and

23  $\{\underline{w}_d\}$  under inversion has been exploited with  $j = j(i) = 2, 1, 4, 3$  for  $i = 1, 2, 3, 4$  respectively,  
 24 for the coordinates  $\underline{w}_\alpha^{(i)}$  listed in Fig. 1 in the main text. The sum above can simply be recast as:

$$\mathcal{P} [\phi_{\underline{k}}(\underline{\xi}|\{\underline{w}_c\}, \Omega)] = \sum_{i=1}^4 e^{-2i\pi(\underline{w}_c^{(i)} + \underline{w}_d^{(j)}) \cdot \underline{k}} \phi_{\underline{k}}(\underline{\xi}|\underline{w}_d^{(j)}, \Omega) = \phi_{\underline{k}}(\underline{\xi}|\{\underline{w}_d\}, \Omega) \quad (2)$$

25 since the sum  $\underline{w}_c^{(i)} + \underline{w}_d^{(j)} = \underline{n}$ , with  $\underline{n}$  integer lattice translation for all  $i, j(i)$ . For the pair  $(a, b)$   
 26 the derivation is straightforward since the lattices generated by  $\{\underline{w}_a\}$  and  $\{\underline{w}_b\}$  are invariant under  
 27 inversion, one thus has:

$$\mathcal{P} [\phi_{\underline{k}}(\underline{\xi}|\{\underline{w}_a\}, \Omega)] = \sum_{i=1}^4 (-1)^{4\underline{w}_a^{(i)} \cdot \underline{k}} \phi_{\underline{k}}(\underline{\xi}|\underline{w}_a^{(i)}, \Omega). \quad (3)$$

28 The parity eigenvalue introduced in the main text, takes values  $e_*(\underline{w}_a^{(i)}, \Gamma) = e_*(\underline{w}_a^{(i)}, Z) = 1$  for  
 29 all  $i$  and  $e_*(\underline{w}_a^{(i)}, \frac{1}{2}Z) = \pm 1$  for  $i \in \{1, 2\}$  or  $i \in \{3, 4\}$  respectively (parity need not be conserved  
 30 along the dispersion curve, since it is not a space group element). By introducing the following  
 31 coefficients:  $c_1 = [1, 1, 1, 1]; c_2 = [1, 1, -1, -1]; c_3 = [1, -1, 1, -1]; c_4 = [1, -1, -1, 1]$ , for  
 32 the linear combinations of BSs  $\phi_{\underline{k}}^{(c_n)}(\underline{\xi}|\{\underline{w}_\alpha\}, \Omega) = \sum_i c_n(i) \phi_{\underline{k}}(\underline{\xi}|\underline{w}_a^{(i)}, \Omega)$ , one has that along the  
 33 dispersion  $\Gamma - Z$  (taking the midpoint as representative wavevector) the statements in Eqs. 2 and  
 34 3 can be recast as:

$$\mathcal{P} [\phi_{\underline{k}}^{(c_n)}(\underline{\xi}|\{\underline{w}_\alpha\}, \Omega)] = \phi_{\underline{k}}^{(c_n)}(\underline{\xi}|\{\underline{w}_\beta\}, \Omega) \text{ for all } n \text{ and with } \alpha = c, d \text{ and } \beta = d, c, \text{ respectively,}$$

$$\mathcal{P} [\phi_{\underline{k}}^{(c_n)}(\underline{\xi}|\{\underline{w}_\alpha\}, \Omega)] = \phi_{\underline{k}}^{(c_j)}(\underline{\xi}|\{\underline{w}_\alpha\}, \Omega) \text{ for } \alpha = a, b \text{ and with } j(n) = 2, 1, 4, 3 \text{ for } n = 1, 2, 3, 4.$$

35 So, in practice the inversion symmetry swaps the sublattices  $\{\underline{w}_c\} \leftrightarrow \{\underline{w}_d\}$  for all  $c_n$ , whereas  
 36 for the BSs @  $\{\underline{w}_a\}, \{\underline{w}_b\}$  the action keeps the sublattices fixed but swaps the coefficients  $c_n \leftrightarrow$   
 37  $c_{n+1}$  for  $n = 1, 3$ . This observation can then help rationalise the transformation properties of  
 38 the lower symmetry BSs under space group operations at the  $\Gamma$ -point reported in Tab. S1: the  
 39 correspondence between WPs  $c$  and  $d$  implies that BSs have to have matching symmetry properties,  
 40 which can be different if the overall symmetry is altered by changing the coefficients  $c_n$ . On the

<sup>41</sup> other hand, the BSs @  $\{\underline{w}_a\}, \{\underline{w}_b\}$  do not show symmetry lowering at the hand of the coefficients  
<sup>42</sup>  $c_n$ , and the full invariance with respect to space group symmetry operations is retained.

Table S1: Transformation symmetries for the Bloch states generated by the linear combinations  $c_i, i = 1 \dots 4$  of  $s$ -GTOs located at the Wyckoff positions  $\underline{w}_\alpha$ ,  $\alpha = a, b, c, d$ .

| BS @                  | $\Gamma_1$           | $\Gamma_2$ | $\Gamma_3$ | $\Gamma_4$ |
|-----------------------|----------------------|------------|------------|------------|
| $\{\underline{w}_a\}$ | $c_1, c_2, c_3, c_4$ | -          | -          | -          |
| $\{\underline{w}_b\}$ | $c_1, c_2, c_3, c_4$ | -          | -          | -          |
| $\{\underline{w}_c\}$ | $c_1$                | $c_3$      | $c_2$      | $c_4$      |
| $\{\underline{w}_d\}$ | $c_1$                | $c_3$      | $c_2$      | $c_4$      |

## <sup>43</sup> 2 Character table and additional plots for the BSs

<sup>44</sup> Character table for  $G_\Gamma$ , the little group at the  $\Gamma$ -point (Tbl.S2) and section in the plane  $\xi_3 = 0$  of  
<sup>45</sup> the BSs considered in the main text (Fig. S1).

Table S2: Character table for  $G_\Gamma$ , the little group at the  $\Gamma$ -point

| Irrep      | $e$ | $m_x$ | $m_z$ | $m_y$ |
|------------|-----|-------|-------|-------|
| $\Gamma_1$ | 1   | 1     | 1     | 1     |
| $\Gamma_2$ | 1   | -1    | -1    | 1     |
| $\Gamma_3$ | 1   | -1    | 1     | -1    |
| $\Gamma_4$ | 1   | 1     | -1    | -1    |

## <sup>46</sup> 3 Additional derivations

### <sup>47</sup> 3.1 Derivative of Bloch state's periodic component

<sup>48</sup> The derivative of the unnormalised periodic component of the Bloch state,  $\tilde{u}_k$ , is reported in Sec.  
<sup>49</sup> 3.2 and it evaluates as:

$$\frac{\partial}{\partial k^\mu} \tilde{u}_k(\underline{\xi} | \underline{w}, \Omega) = \frac{\partial}{\partial k^\mu} \left( e^{-2i\pi \underline{\xi} \cdot \underline{k}} \tilde{\phi}_k(\underline{\xi} | \underline{w}, \Omega) \right) = -2i\pi (\underline{e}^\mu, \underline{\xi} + \underline{w}) e^{-2i\pi \underline{\xi} \cdot \underline{k}} \tilde{\phi}_k(\underline{\xi} | \underline{w}, \Omega) + e^{-2i\pi \underline{\xi} \cdot \underline{k}} \tilde{\phi}'_{\underline{e}^\mu, k}(\underline{\xi} | \underline{w}, \Omega)$$

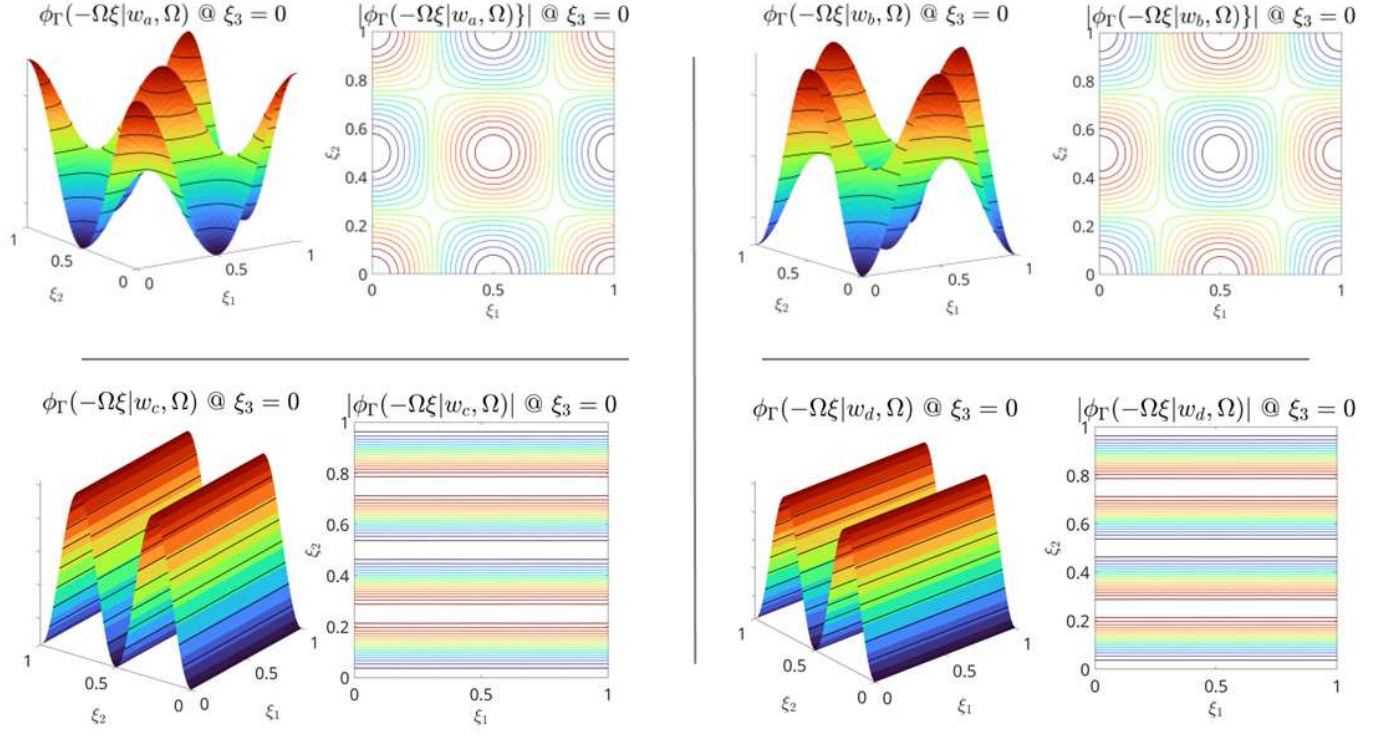


Figure S1: Bloch states @  $\{\underline{w}_\alpha\}$ ,  $\alpha = a, b, c, d$ . Each panel shows the real part (left) and the absolute value of the BS in the plane  $\xi_3 = 0$ .

50 which can then be replaced in the corresponding expression for the normalised  $u_k$ :

$$\frac{\partial}{\partial k^\mu} u_{\underline{k}}(\underline{\xi} | \underline{w}, \Omega) = \left( \frac{\partial}{\partial k^\mu} N_{\underline{k}} \right) \tilde{u}_{\underline{k}}(\underline{\xi} | \underline{w}, \Omega) + N_{\underline{k}} \frac{\partial}{\partial k^\mu} \tilde{u}_{\underline{k}}(\underline{\xi} | \underline{w}, \Omega)$$

51 with the assumption leading to Eq. 3 in the main text, the derivative above reads:

$$\frac{\partial}{\partial k^\mu} u_{\underline{k}}(\underline{\xi} | \underline{w}, \tau \text{diag}(a^2, b^2, c^2)) = \left\{ - \left[ 2i\pi(\underline{e}^\mu, \underline{\xi} + \underline{w}) + \frac{1}{2} \frac{\vartheta'(\underline{k}^\mu | \omega^\mu)}{\vartheta(\underline{k}^\mu | \omega^\mu)} \right] \phi_{\underline{k}}(\underline{\xi} | \underline{w}, \tau \text{diag}(a^2, b^2, c^2)) + \phi'_{\underline{e}^\mu, \underline{k}}(\underline{\xi} | \underline{w}, \tau \text{diag}(a^2, b^2, c^2)) \right\}$$

52 where  $\omega^\mu = \frac{1}{2}\tau(\underline{e}^\mu, \text{diag}(a^2, b^2, c^2))$  is the component of the period matrix along the direction in  
53 which the derivative is evaluated.

54 Next I am reporting the evaluation of the matrix element of the Berry connection, given in Eq.

55 4 in the main text.

$$\left\langle u_{\underline{k}} \left| \frac{\partial}{\partial k^\mu} u_{\underline{k}} \right. \right\rangle = N_{\underline{k}}^2 \int_{\mathcal{U}} d\underline{\xi} \tilde{\phi}_{-\underline{k}}(\underline{\xi} | \underline{w}, \tau \text{diag}(a^2, b^2, c^2)) (-2\pi i) (\underline{e}^\mu, \underline{\xi} + \underline{w}) \tilde{\phi}_{\underline{k}}(\underline{\xi} | \underline{w}, \tau \text{diag}(a^2, b^2, c^2))$$

(4)

$$- \frac{1}{2} N_{\underline{k}}^2 \frac{\vartheta'(k^\mu | \omega)}{\vartheta(k^\mu | \omega)} \int_{\mathcal{U}} d\underline{\xi} \tilde{\phi}_{-\underline{k}}(\underline{\xi} | \underline{w}, \tau \text{diag}(a^2, b^2, c^2)) \tilde{\phi}_{\underline{k}}(\underline{\xi} | \underline{w}, \tau \text{diag}(a^2, b^2, c^2))$$

(5)

$$+ N_{\underline{k}}^2 \int_{\mathcal{U}} d\underline{\xi} \tilde{\phi}_{-\underline{k}}(\underline{\xi} | \underline{w}, \tau \text{diag}(a^2, b^2, c^2)) \tilde{\phi}'_{\underline{e}^\mu, \underline{k}}(\underline{\xi} | \underline{w}, \tau \text{diag}(a^2, b^2, c^2)).$$

(6)

56 The integral over the unit cell  $\mathcal{U}$  in Eq.5 above evaluates to:

$$\int_{\mathcal{U}} d\underline{\xi} \tilde{\phi}_{-\underline{k}}(\underline{\xi} | \underline{w}, \tau \text{diag}(a^2, b^2, c^2)) \tilde{\phi}_{\underline{k}}(\underline{\xi} | \underline{w}, \tau \text{diag}(a^2, b^2, c^2)) = (abc)^{-1} \left( \frac{\pi}{2\beta} \right)^{3/2} \prod_{\mu=1}^3 \vartheta(k^\mu | \omega^\mu),$$

(7)

57 whereas the sum of the remaining terms in Eqs. 4, 6 is:

$$N_{\underline{k}}^2 \int_{\mathcal{U}} d\underline{\xi} \tilde{\phi}_{-\underline{k}}(\underline{\xi} | \underline{w}, \tau \text{diag}(a^2, b^2, c^2)) \left[ \tilde{\phi}'_{\underline{e}^\mu, \underline{k}}(\underline{\xi} | \underline{w}, \tau \text{diag}(a^2, b^2, c^2)) - 2\pi i (\underline{e}^\mu, \underline{\xi} + \underline{w}) \tilde{\phi}_{\underline{k}}(\underline{\xi} | \underline{w}, \tau \text{diag}(a^2, b^2, c^2)) \right]$$

(8)

58 which can be evaluated straightforwardly if one recognises the expression for the  $p$ -GTO BS:<sup>S2</sup>

59  $-2\pi i \tilde{\phi}_{\underline{k}}^{(p_\mu)} = \tilde{\phi}'_{\underline{e}^\mu, \underline{k}} - 2\pi i (\underline{e}^\mu, \underline{\xi}) \tilde{\phi}_{\underline{k}}$ . Then one has that the term in Eq. 8 above evaluates as:

$$N_{\underline{k}}^2 \int_{\mathcal{U}} d\underline{\xi} \tilde{\phi}_{-\underline{k}}(\underline{\xi} | \underline{w}, \tau \text{diag}(a^2, b^2, c^2)) \tilde{\phi}_{\underline{k}}^{(p_\mu)}(\underline{\xi} | \underline{w}, \tau \text{diag}(a^2, b^2, c^2))$$

$$- 2\pi i N_{\underline{k}}^2 (\underline{e}^\mu, \underline{w}) \int_{\mathcal{U}} d\underline{\xi} \tilde{\phi}_{-\underline{k}}(\underline{\xi} | \underline{w}, \tau \text{diag}(a^2, b^2, c^2)) \tilde{\phi}_{\underline{k}}(\underline{\xi} | \underline{w}, \tau \text{diag}(a^2, b^2, c^2))$$

60 Recalling that (see Sec. 3.3 below)  $\langle \tilde{\phi}_{\underline{k}} | \tilde{\phi}_{\underline{k}}^{(p_\mu)} \rangle = 0$  one obtains:

$$\left\langle u_{\underline{k}} \left| \frac{\partial}{\partial k^\mu} u_{\underline{k}} \right. \right\rangle = -\frac{1}{2} (abc)^{-1} \left( \frac{\pi}{2\beta} \right)^{3/2} N_{\underline{k}}^2 \vartheta(k^\nu | \omega^\nu) \vartheta(k^\lambda | \omega^\lambda) [\vartheta'(k^\mu | \omega^\mu) + 4\pi i (\underline{e}^\mu, \underline{w}) \vartheta(k^\mu | \omega^\mu)]$$

61 By replacing the expression for the normalisation constant:  $N_k^2 = (abc) \left(\frac{2\beta}{\pi}\right)^{3/2} [\vartheta(k^\mu|\omega^\mu) \vartheta(k^\nu|\omega^\nu) \vartheta(k^\lambda|\omega^\lambda)]^{-1}$ ,

62 Eq. 4 in the main text is obtained.

### 63 3.2 Derivative of the periodic component of the Bloch states

64 In this section I report the derivation of the equality:

$$\frac{\partial}{\partial k^\mu} \tilde{\phi}_{\underline{k}}(\underline{\xi}|\underline{w}, \Omega) = \frac{\partial}{\partial k^\mu} \left( e^{-2i\pi \underline{\xi} \cdot \underline{k}} \tilde{\phi}_{\underline{k}}(\underline{\xi}|\underline{w}, \Omega) \right) = -2i\pi(\underline{e}^\mu, \underline{\xi} + \underline{w}) e^{-2i\pi \underline{\xi} \cdot \underline{k}} \tilde{\phi}_{\underline{k}}(\underline{\xi}|\underline{w}, \Omega) + e^{-2i\pi \underline{\xi} \cdot \underline{k}} \tilde{\phi}'_{\underline{e}^\mu, \underline{k}}(\underline{\xi}|\underline{w}, \Omega). \quad (9)$$

65 The statement can be derived easily by applying the following:

$$\frac{\partial}{\partial k^\mu} \tilde{\phi}_{\underline{k}}(\underline{\xi}|\underline{w}, \Omega) = \tilde{\phi}'_{\underline{e}^\mu, \underline{k}}(\underline{\xi} - \underline{w}|0, \Omega), \quad (10)$$

66 and the translational invariance reported in Eq.(10) of ref.:<sup>S2</sup>

$$\tilde{\phi}'_{\underline{e}, \underline{k}}(\underline{\xi}|\underline{w}, \Omega) = 2\pi i(\underline{e}, \underline{w}) \tilde{\phi}_{\underline{k}}(\underline{\xi}|\underline{w}, \Omega) + \tilde{\phi}'_{\underline{e}, \underline{k}}(\underline{\xi} - \underline{w}|0, \Omega).$$

67 Eq.10 can then be immediately obtained as follows:

$$\begin{aligned} \frac{\partial}{\partial k^\mu} \tilde{\phi}_{\underline{k}}(\underline{\xi}|\underline{w}, \Omega) &= e^{i\pi \underline{\xi} \cdot \Omega \underline{\xi}} e^{-2\pi i \underline{w} \cdot \underline{k}} \left( D_{\underline{e}^\mu} \left[ \vartheta \begin{bmatrix} \underline{w} \\ 0 \end{bmatrix} (\underline{k} - \Omega \underline{\xi}|\Omega) \right] - 2\pi i(\underline{e}^\mu, \underline{w}) \vartheta \begin{bmatrix} \underline{w} \\ 0 \end{bmatrix} (\underline{k} - \Omega \underline{\xi}|\Omega) \right) \\ &= \tilde{\phi}'_{\underline{e}^\mu, \underline{k}}(\underline{\xi}|\underline{w}, \Omega) - 2\pi i(\underline{e}^\mu, \underline{w}) \tilde{\phi}_{\underline{k}}(\underline{\xi}|\underline{w}, \Omega), \end{aligned}$$

68 and by applying the chain rule for the derivatives.

### 69 3.3 Bloch states from s- and p- GTOs are orthogonal

70 The expression for the overlap integral of  $s$ - and  $p$ -BSs in one cartesian dimension reads, by setting  
 71 the lattice constant to 1, as:

$$S_k^{(0,1)} = \langle \tilde{\phi}_k^{(0)} | \tilde{\phi}_k^{(1)} \rangle = \int_0^1 dx \tilde{\phi}_{-k}^{(0)}(x) \left[ x \tilde{\phi}_k^{(0)}(x) - \frac{1}{2i\pi} \frac{d}{dx} \tilde{\phi}_k^{(0)}(x) \right],$$

72 where the  $s$ - and  $p$ - Bloch states have been indicated by the respective quantum number and the  
 73 expression for the  $\tilde{\phi}_k^{(1)}$  has been given in Eq. 12 of ref.<sup>S2</sup>. The dependence on the Wyckoff position  
 74 has been omitted, since the integral is insensitive to it, as long as states arise from GTOs on the  
 75 same Wyckoff position. By plugging in the appropriate definitions, the integral becomes:

$$S_k^{(0,1)} = \sum_{m,n \in \mathbb{Z}} e^{2i\pi k(n-m)} e^{-\frac{\beta}{2}(n-m)^2} \int_0^1 dx (x-n) e^{-2\beta(x-\frac{1}{2}(m+n))^2} \quad (11)$$

$$= \sum_{s,n \in \mathbb{Z}} e^{-2i\pi ks} e^{-\frac{\beta}{2}(-s)^2} \int_0^1 dx (x-n) e^{-2\beta(x-\frac{s}{2}-n)^2}. \quad (12)$$

76 By means of a change of variable, it is possible to carry out the summation over the  $n$  index to  
 77 obtain:

$$S_k^{(0,1)} = \sum_{s \in \mathbb{Z}} e^{-2i\pi ks} e^{-\frac{\beta}{2}(-s)^2} \int_{-\infty}^{+\infty} dy y e^{-2\beta(y-\frac{s}{2})^2} = 0, \quad (13)$$

78 where the last equality follows on the ground of parity.

## 79 References

80 (S1) Mumford, D. *Tata Lectures on Theta I*; Birkh auser, 1983.

81 (S2) Maggio, E. Exploiting  $\vartheta$ -functions for the identification of topological materials. *AIP Ad-*  
 82 *vances* **2025**, 15, 085107.